

Supplementary Information

Molecular Structure of 2a,b and 3a,b

Annotation to the eclipsed/staggered rotamers of the $\{M(\text{CO})_5\}$ fragments

Two opposite carbonyl ligands of the pentacarbonyl fragments in the trinuclear complexes adopt a “staggered” configuration with respect to the terminal butoxy substituents at both tin atoms (see figure 1), which has the consequence that two carbonyl ligands are in an “eclipsed” orientation with the bridging O^tBu substituents. The same “staggered” conformation with respect to the tert. butoxy groups and the “eclipsed” orientation of the carbonyl ligands is found in the tetranuclear complexes for one of the two pentacarbonyl groups. The second $\{M(\text{CO})_5\}$ moiety adopts an “eclipsed” conformation with the tert. butoxy ligands at tin. Two torsion angles *cis*-(CO)-M-Sn-(term-O) are 0.00° due to the mirror plane, which is perpendicular to the Sn₂O₂ plane. As consequence, the tin-chromium bond lengths in **3b** are slightly different: Sn1-Cr1_{staggered}: 2.60(4) Å; Sn2-Cr2_{eclipsed}: 2.62(3) Å.

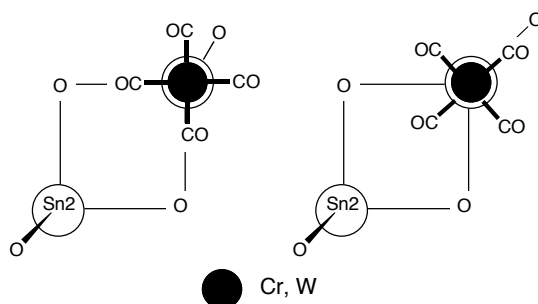


fig. 1: Schematic drawing of the staggered (left) and eclipsed (right) rotamere with respect to the CO/term. O^tBu arrangement exemplified with the trinuclear complexes. View perpendicular to the Sn₂O₂ plane.

Relationship between bond angle and bond length in the Sn₂O₂ ring

A plot of the *endohedral* bond angle (μ -O)-Sn_M-(μ -O) against the Sn_M-(μ -O) bond length at the co-ordinated tin atom (fig. 2) shows a correlation: the trinuclear complexes are found in the short bond-obtuse angle region, whereas the tetranuclear complexes are found in the long bond length-acute angle region.

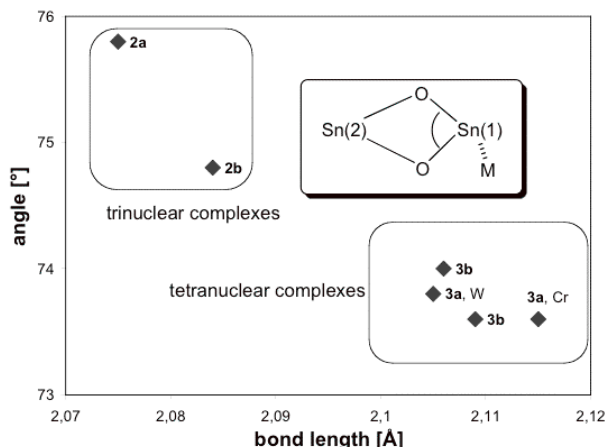


fig. 2: Change of $(\mu\text{-O})\text{-Sn}_M\text{-(}\mu\text{-O)}$ bond angle and $\text{Sn}_M\text{-(}\mu\text{-O)}$ bond length in the complexes **2a**, **2b**, **3a** and **3b**.

X-ray molecular structure and NMR spectra

Relationship between J_{SnSn} coupling constant and bond angle $(\mu\text{-O})\text{-Sn}_M\text{-(}\mu\text{-O)}$

Relationships between electronegativity of the substituents, co-ordination deshielding, chemical shifts and coupling constants with structural parameters have been discussed occasionally.^[1] There is the well-known increase of the coupling constant with higher s-character for the atomic orbitals in e.g. carbon-hydrogen coupling constants.^[2] A sort of indicator for the hybridisation state of the orbitals at tin is provided by the bond angle $(\mu\text{-O})\text{-Sn-(}\mu\text{-O)}$: the $^2J_{\text{Sn-Sn}}$ coupling between the tin atoms increases with larger angle (see figure 3). Although a clear correlation cannot be assessed, the trend is distinct.

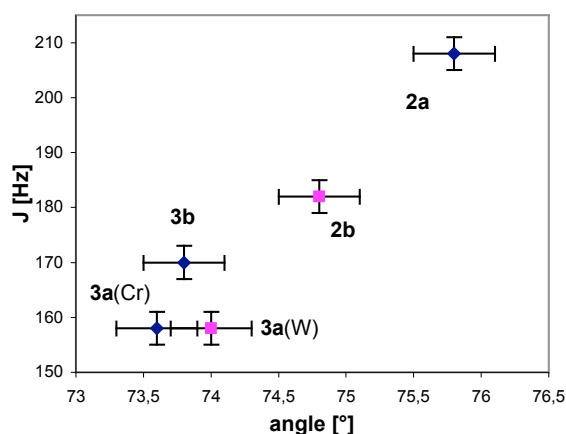


fig. 3: Coupling constant $^2J_{\text{Sn-Sn}}$ from solution NMR against the angle $(\mu\text{-O})\text{-Sn-(}\mu\text{-O)}$ in the solid state structure of the complexes **2a**, **2b**, **3a**, **3b**, (errors taken as ± 3 Hz for J and 0.3° for the angle).

Relationship between ^{13}C chemical shift and (transition metal)-C bond length for the $\text{M}(\text{CO})_5$ fragments

An increasing π -backdonating ability of the central metal atom should correlate with ^{13}C deshielding.^[1] Due to high uncertainties in the carbon-oxygen distances observed from the X-ray structure determinations, such a correlation could not be established. However, the degree of back bonding is also documented in the bond lengths $\text{M}-\underline{\text{C}}\text{O}$ between the respective kind of carbon atom (*cis-/trans*-CO) and the central metal. This crystallographic measure correlates well with the spectroscopic ^{13}C chemical shifts: the shorter the bond, the higher the absorption frequency. This is illustrated for the chromium complexes in figure 10; the two tungsten complexes show the same tendency (*trans*-CO/*cis*-CO: **2b** (1.90(2) Å, 199.5 ppm / 2.00(2) Å, 197.6 ppm), **3a** (2.01(2) Å, 197.3 ppm / 2.04(2) Å, 197.0 ppm)).

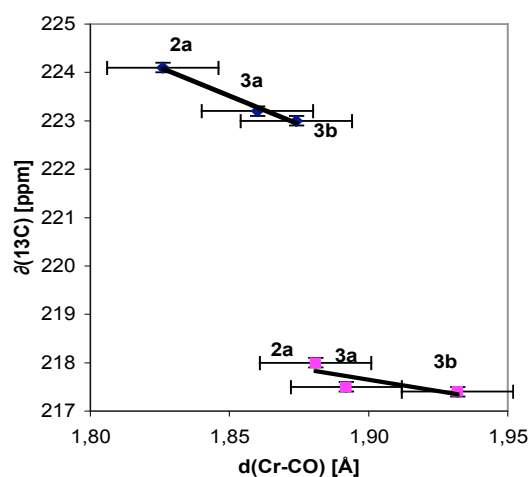


fig. 4: Correlation between carbon chemical shifts and bond lengths Cr-(CO) for **2a**, **3a** and **3b** (top: *trans*-CO, bottom: *cis*-CO; errors taken as 0.02 ppm and 0.1 Å).

NMR spectra

Overview of the ^{13}C NMR values for the complexes at r.t.

	δ (^{13}C) [ppm]; J [Hz]							
	CO , ($^1J_{\text{C-W}}$), ($^2J_{\text{C-Sn}}$)		O^tCMe_3 , ($J_{\text{C-Sn}}$)			$\text{O}^t\text{C}(\text{CH}_3)_3$, ($J_{\text{C-Sn}}$)		
	<i>trans</i>	<i>cis</i>	terminal		bridging	terminal		bridging
2a	224.1 {69.4}	218.0 {125.2}	73.6 (6.3)	72.1 (4.9)	77.9 (5.9)	35.7 (25)	34.7 (10,br)	33.1 (22.8)
2b	199.3 (164) {128}	197.6 (124) {61/64}	73.8	72.2 (10)	78.1 (br)	35.7 (24)	34.8	33.4 (22/11)
3a , Cr	223.0	217.4 {121}		74.2	80.7		34.5	32.7 (10)
W	197.3	197.0 (124) {56}	74.3 (9)			34.6 (18)		
3b	223.2	217.5 {69}	74.3		80.7	34.5		32.7
3c	197.7	197.1	74.3		80.9	34.6		33.0

tab. 1: $^{13}\text{C}\{^1\text{H}\}$ NMR spectra for the complexes $[\{(\text{OC})_5\text{M}\}_n\{(\text{OC})_5\text{M}'\}_m\{\text{Sn}_2(\text{O}^t\text{Bu})_4\}]$ ($n = 1, m = 0, \text{M} = \text{Cr}$ (**2a**), W (**2b**); $n = 1, m = 1, \text{M} = \text{Cr}, \text{M}' = \text{W}$ (**3a**), $\text{M} = \text{M}' = \text{Cr}$ (**3b**), W (**3c**)) in benzene solution.

Temperature variable ^1H NMR spectroscopy*Drift of chemical shift in complexes 2a, 2b, 3b*

In the ^1H NMR spectra of **2a**, **2b** and **3b** all the signals show a pronounced drift of the chemical shift with temperature. Interestingly, this drift behaviour is very different for the signals: while the two low field resonances (integral ratio 1:1) in the spectra of **2a** and **2b** move to high field with increasing temperature with a parabolic curvature, the high field signal (rel. integral 2) moves strictly linearly to low field (see figure 5). While the chemical shift of the signals for the bridging O^tBu substituents in both complexes are very similar (according to absolute values and slope), the low field signal is more deshielded in the tungsten than in the chromium derivative, while with the intermediate signal, the situation is reversed. The low field signal in both complexes shows a stronger drift difference than the intermediate singlet, and therefore is ascribed to the O^tBu substituent at the co-ordinated tin atom. This is also in accord with the expected deshielding on co-ordination.

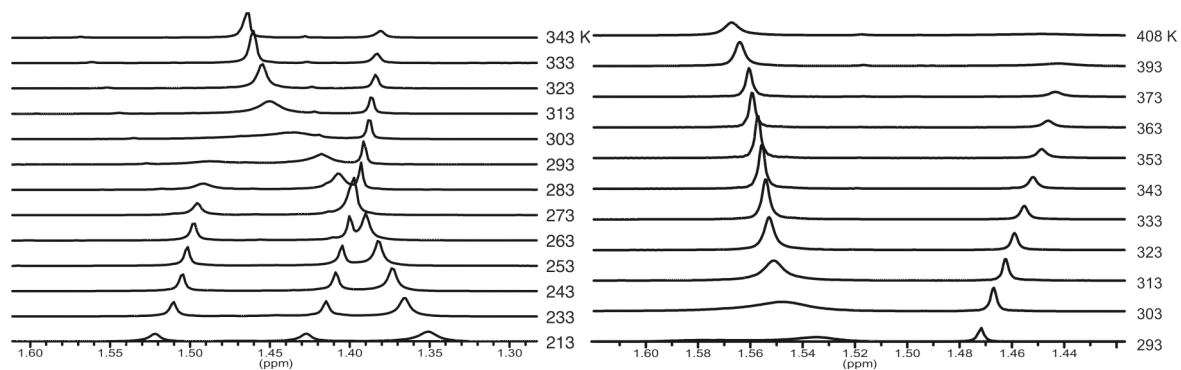


fig. 5: Temperature variable ^1H NMR spectra of **2b** in the range of a) 213-343 K (d_8 -toluene); b) 293-408 K (d_{10} -xylene).

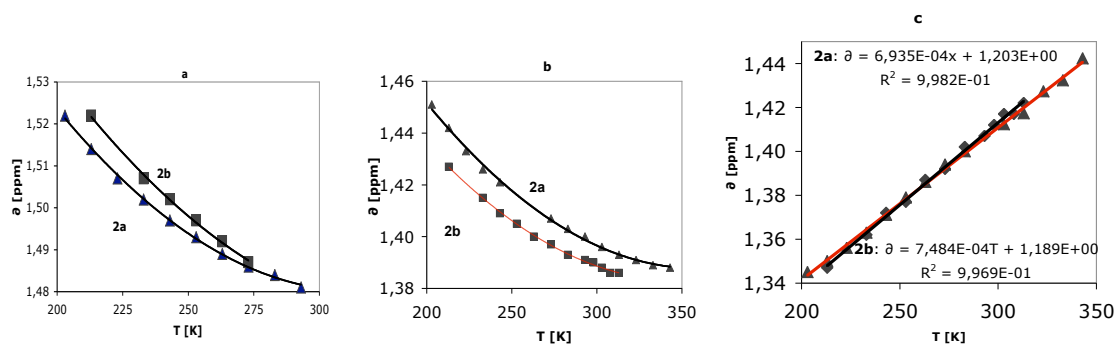


fig. 6: Drift of chemical shift in the ^1H NMR spectra of **2a** (▲) and **2b** (■) (a/b/c: low/middle/high field singlet; integral 1:1:2).

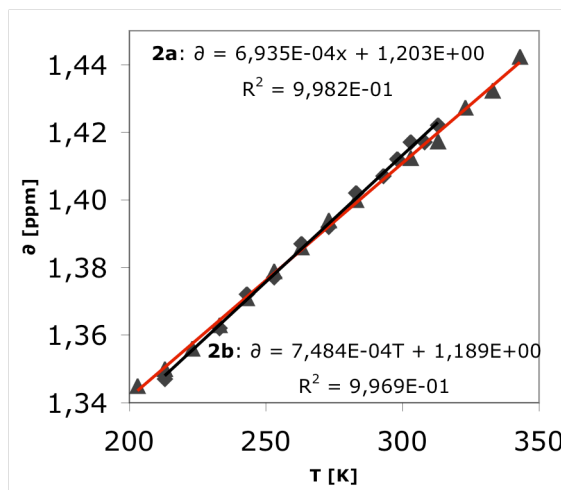


fig. 6: Drift of chemical shift in the ^1H NMR spectra of **2a** (▲) and **2b** (■) (high field singlet; rel. integral 2).

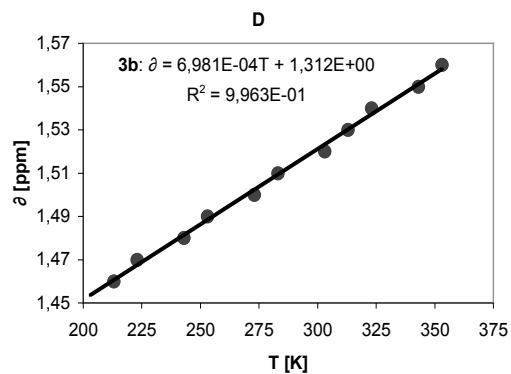


fig. 7: Drift of chemical shift for the low field (rel. intensity 2) signal in the ^1H NMR spectra of **3b**.

For the tetranuclear **3b**, the high field signal is basically unchanged over the temperature range (213 K: 1.42 ppm; 353 K: 1.44 ppm), while the low field signal shows a linear increase of the chemical shift value with temperature (see figure 13). The slope is equal to that of the signal at highest field (high temperature) in the trinuclear complexes ($7.0 \cdot 10^{-4}$ ppm/K (**3b**) vs. $6.9 \cdot 10^{-4}$ (**2a**) and $7.5 \cdot 10^{-4}$ ppm/K (**2b**)). This makes the attribution to the bridging O^tBu substituents very probable, although the relative δ -values of the bridging and terminal O^tBu groups would then be reversed with respect to the trinuclear and hetero-bis(transition metal) complexes.

Temperature variable ^{13}C NMR spectroscopy

Drift of chemical shift in the carbonyl region of complex **2b**

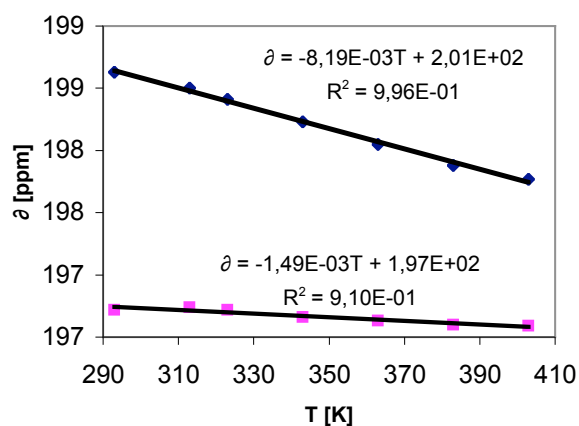


fig. 8: Chemical shift δ [ppm] over temperature in the ^{13}C NMR spectra of **2b** in xylene (CO-region; top: *trans*-CO, bottom: *cis*-CO).

Drift of chemical shift in the alkyl region of complex **2b**

In the quaternary carbon region, with increasing temperature, a weak shielding effect is observed for that terminal O^tBu , which is incorporated in the exchange only at high temperature, whereas the respective methyl carbon resonance shift is basically unchanged (see figure 9). The bridging ^tBu group resonance in the methyl C region is slightly deshielded.

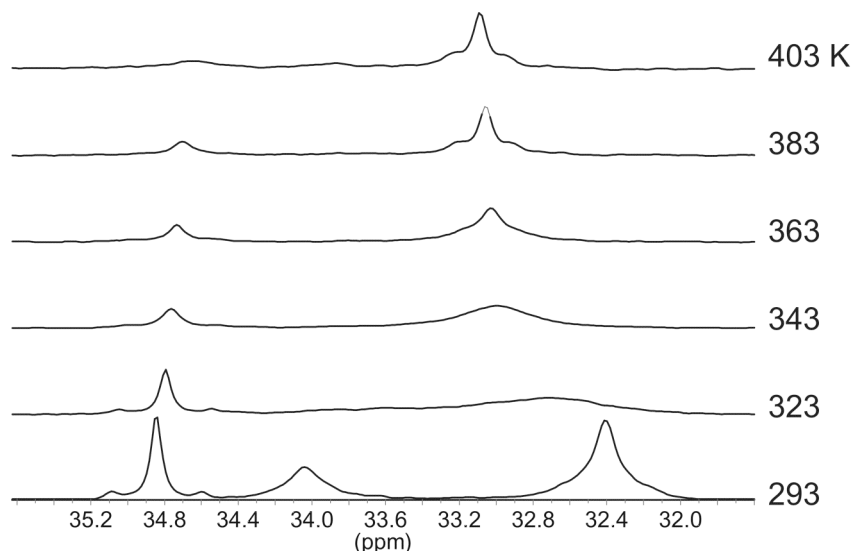


fig. 9: $^{13}\text{C}\{^1\text{H}\}$ spectra of **2b** in the methyl region between 293 and 403 K (xylene).

1. J. Mason (ed), *Multinuclear NMR*, Plenum Press, NY, **1987**, 639 pp.
2. M. Hesse, H. Meier, B. Zeeh, *Spektroskopische Methoden in der organischen Chemie*, Georg Thieme Verlag, Stuttgart, New York, 4. ed., **1991**, 336 pp.